Problems with a popular thick plate element and the development of an improved thick plate element

Cheng Y.M.[†]

Department of Civil and Structural Engineering, Hong Kong Polytechnic University, Hong Kong

Law C.W.

Housing Department, Hong Kong SAR Government, Hong Kong

Abstract. Some unreasonable results from the use of a popular thick plate element are discovered from the analysis of a raft foundation and a pile cap in Hong Kong. To overcome the problems, the authors have developed a new shear deformable beam which can be extended to a general quadrilateral shear deformable plate. The behaviour of this new element under several interesting cases is investigated, and it is demonstrated that the new element possesses very high accuracy under different depth/span ratios, and the results from this new element are good even for a coarse mesh.

Keywords: thick plate; shear deformation; finite element.

1. Introduction

Pile caps, transfer plates and raft foundations are typical structures which are important and expensive thick plates. These structures are so thick that shear deformation cannot be neglected, and the use of Kirchhoff plate theory will be less satisfactory. For the past twenty years, many thick plate elements have been developed and are used by engineers (Urugal 1999, Reddy 2000, Szilard 2004) and extensive treatment of various thick plate elements has been covered by Zienkiewicz and Taylor (2000) and many others. The popular classical quadrilateral elements include the Q4, Q4-R, DKQ by Katili (1993), MITC4 by Bathe and Dvorkin (1985) and MITC7 and MITC9 by Bathe *et al.* (1989), the stabilized MITC elements by Lyly and Stenbergy (1998), the one point integration with stabilization matrix by Hughes (1986, 1987). The popular classical triangular elements include the T3, T3-R, DST-BL by Batoz and Lardeur (1989). One simple and straightforward approach is proposed by Ibrahimbegovic (1992, 1993). Ibrahimbegovic utilized the Timoshenko's beam formulas to determine the deflection, rotations and shear strain along element sides, and then constructed three quadrilateral thin-thick plate elements PQ1, PQ2 and PQ3 by using mixed interpolation method. Soh *et al.* (2001) provided another set of locking-free Timoshenko's beam formulas with the development of a new thin/thick plate element (ARS-Q12). ARS-Q12 has no

† Ph.D., Corresponding author, E-mail: ceymchen@polyu.edu.hk

numerical problem and exhibits good performance for both thin and thick plates. The same Timoshenko's beam formulas also appeared in the constructions of elements RDKQM (full integration), DKTM and RDKTM (one point integration re-constitution shear-strain element) by Chen and Cheung (2000, 2001). Sheikh and Dey (2001) proposed a new triangular element based on the Reissner-Mindlin's plate theory for thin and thick plate. This element may have any arbitrary triangular shape, which has the advantage of analyzing plates of any geometry. Gruttmann and Wagner (2004) utilized a Hellinger-Reissner functional with independent displacements, rotations and stress resultants and proposed a new quadrilateral Reissner-Mindlin plate element with 12 degrees of freedom. Gruttmann and Wagner (2004) adopted a formulation close to that by Hughes (1986, 1987) by using a stabilizing matrix. Cen *et al.* (2006) used the quadrilateral area co-ordinate method to formulate a new quadrilateral element, named AC-MQ4. This element is free of shear locking and is insensitive to mesh distortion. Ozdemir *et al.* (2007) have proposed 8 and 17 nodes shear locking free elements based on purely the use of higher order polynomial without any other special treatment, and these elements can be formed easily by classical finite element method. These 8 nodes element produces a relatively poor result for coarse mesh while the 17 nodes element can produce a very good result even for a coarse mesh. Ozgan and Daloglu (2007) have proposed four and eight node elements (PBQ4 and PBQ8) based on the classical Mindlin plate theory. Abdalla and Ibrahim (2007) have also proposed a discrete Reissner-Mindlin thick plate element for geometrical non-linear problem. Among the elements mentioned, the thick plate element by Ibrahimbegovic (1993) (termed as IB element in later study) is one of the most popular thick plate elements currently adopted by some commercial programs and many engineers for thick plate analysis in many countries. The four node IB element can suit the loadings and structures easily compared with other higher order elements, and the element is widely adopted for engineering use. The authors have recently discovered some problems of this element from several real jobs which have generally been overlooked in the past, though this element has been used for the analysis of many thick plate structures for a long time.

In this paper, the limitations of the IB element will be demonstrated by several interesting cases originated from two real jobs in Hong Kong. In view of the limitations of the element, a new shear deformable beam element which is free from shear locking is developed, based on which a new quadrilateral thick plate element "PLATE" is formulated in this paper. It can be demonstrated that "PLATE" can provide a good accuracy and convergence, particularly for coarse mesh problems. The new thick plate is formulated initially as a rectangular element and then later extended to a general quadrilateral element which is more useful to irregular structures.

2. Formulation of a new shear deformable beam free from shear locking

Most of the thick plate elements are based on the extension of shear deformable beam where shear strain is included in the computation of displacement. The relationship among the parameters (i) out-of-plane displacement ω; (ii) out-of-plane rotation ψ; (iii) out-of-plane shear strain γ for a shear deformable beam is illustrated in Fig. 2. The main differences in the formulations between different researchers are the order of polynomial used for the finite element formulation (Bathe *et al.* 1985, Hughes *et al.* 1986, Jirousek *et al.* 1995, Zienkiewicz 1991, Sze 2002) and the methods to determine the polynomial coefficients. In the present formulation for the beam as shown in Figs. 1 and 2, the deflection ω is represented by a 3rd order polynomial. The rotation ψ would then be a 2nd
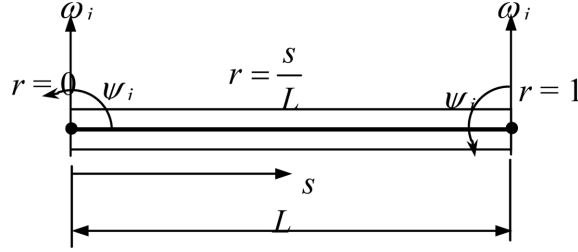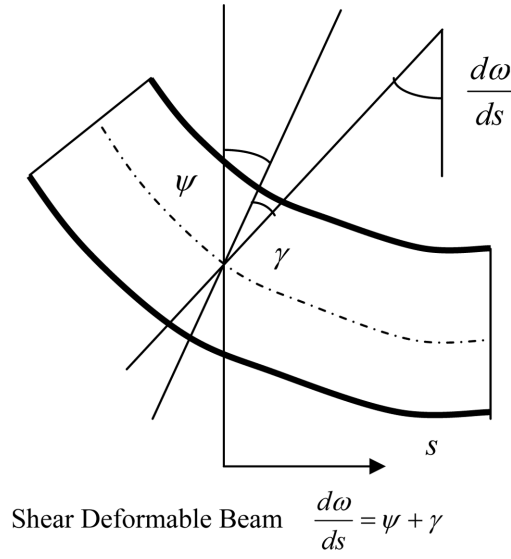
Fig. 1 Symbols for thick beam formulation

Shear Deformable Beam $\quad \dfrac{d\omega}{ds} = \psi + \gamma$

Fig. 2 Relationship among $\omega;\ \psi,\ \gamma$ for shear deformable beam

order polynomial. The coefficients and in Eqs. (1) and (2) are constants to be determined from the boundary conditions and energy minimization. r is a normalized dimensionless distance given by $r = s/L$ which lies in the range of 0 to 1.

$$\omega = \alpha_0 + \alpha_1 r + \alpha_2 r^2 + \alpha_3 r^3 \tag{1}$$

$$\psi = \beta_0 + \beta_1 r + \beta_2 r^2 \tag{2}$$

As illustrated in Fig. 2, the angular rotation at any section is the combined action of the bending and shear deformation given by

$$\frac{d\omega}{ds} = \frac{1}{L}\frac{d\omega}{dr} = \psi + \gamma \tag{3}$$

The shear strain within this short segment of beam (shear force is constant) is a constant term γ_0 given by

$$\gamma = \gamma_0 \tag{4}$$

Making use of the boundary conditions at $r = 0$, $\omega = \omega_i$, $\psi = \psi_i$ and at $r = 1$, $\omega = \omega_j$, $\psi = \psi_j$; α_0, α_1, β_0, β_1 in Eqs. (1) and (2) can be expressed in terms of the deflections ω_i and ω_j at the two ends of the beam so that Eq. (1) and Eq. (2) can be rewritten as

$$\omega = (1 - r)\omega_i + r\omega_j + r(-1 + r)\alpha_2 + r(-1 + r^2)\alpha_3 \tag{5}$$

and
$$\psi = \psi_i + (\psi_j - \psi_i - \beta_2)r + \beta_2 r^2 \tag{6}$$

Eq. (3) can now be rewritten as

$$\frac{d\omega}{dr} = L(\psi + \gamma) = -\omega_i + \omega_j + (-1 + 2r)\alpha_2 + (-1 + 3r^2)\alpha_3 \tag{7}$$

Substituting $r = 0$ and $r = 1$ with $\psi = \psi_i$ and $\psi = \psi_j$ in Eq. (7) and solving gives

$$\alpha_2 = -3\omega_i + 3\omega_j - 2L\psi_i - L\psi_j - 3L\gamma_0 ; \quad \alpha_3 = 2\omega_i - 2\omega_j + L\psi_i + L\psi_j + 2L\gamma_0 \tag{8}$$

Back-substituting Eq. (8) into Eq. (5) and re-arranging gives

$$\omega = (1 - r)^2(1 + 2r)\omega_i + r^2(3 - 2r)\omega_j + Lr(1 - r)^2\psi_i + Lr^2(-1 + r)\psi_j + Lr(1 - r)(1 - 2r)\gamma_0 \tag{9}$$

Differentiation of Eq. (9) with respect to s where $s = Lr$ gives

$$\frac{1}{L}\frac{d\omega}{dr} = \frac{-6r + 6r^2}{L}\omega_i + \frac{6r - 6r^2}{L}\omega_j + (1 - 4r + 3r^2)\psi_i + (-2r + 3r^2)\psi_j + (1 - 6r + 6r^2)\gamma_0 \tag{10}$$

Put Eqs. (6), (10) into Eq. (3)

$$\frac{-6r + 6r^2}{L}\omega_i + \frac{6r - 6r^2}{L}\omega_j + (1 - 4r + 3r^2)\psi_i + (-2r + 3r^2)\psi_j + (1 - 6r + 6r^2)\gamma_0$$

$$= (1 - r)\psi_i + r\psi_j + r(-1 + r)\beta_2 + \gamma_0 , \text{ or}$$

$$r(-1 + r)\beta_2 = \frac{-6r + 6r^2}{L}\omega_i + \frac{6r - 6r^2}{L}\omega_j + (-3r + 3r^2)\psi_i + (-3r + 3r^2)\psi_j + (-6r + 6r^2)\gamma_0 \tag{11}$$

β_2 is now determined from Eq. (11) so that Eq. (6) can be re-written as

$$\psi = \frac{6r}{L}(-1 + r)\omega_i + \frac{6r}{L}(1 - r)\omega_j + (1 - 4r + 3r^2)\psi_i + r(-2 + 3r)\psi_j + 6r(-1 + r)r_0 \tag{12}$$

Bending energy U_B per unit width of the shear deformable beam is

$$U_B = \int_0^L \frac{M^2}{2EI}dx = \frac{EIL}{2}\int_0^1 \left(\frac{M}{EI}\right)^2 dr = \frac{EIL}{2}\int_0^1 \kappa^2 dr = \frac{Et^3 L}{12} \frac{}{2}\int_0^1 \left(-\frac{d\psi}{Ldr}\right)^2 dr \tag{13}$$

where κ is the curvature of deflection given by $\kappa = -\dfrac{d\psi}{ds} = -\dfrac{1}{L}\dfrac{d\psi}{ds}$. From Eq. (12)

$$\frac{d\psi}{Ldr} = \frac{-6 + 12r}{L^2}\omega_i + \frac{6 - 12r}{L^2}\omega_j + \frac{-4 + 6r}{L}\psi_i + \frac{-2 + 6r}{L}\psi_j + \frac{-6 + 12r}{L}\gamma_0$$

$$= \left(\frac{-6}{L^2}\omega_i + \frac{6}{L^2}\omega_j + \frac{-4}{L}\psi_i + \frac{-2}{L}\psi_j + \frac{-6}{L}\gamma_0\right) + \left(\frac{12}{L^2}\omega_i + \frac{-12}{L^2}\omega_j + \frac{6}{L}\psi_i + \frac{6}{L}\psi_j + \frac{12}{L}\gamma_0\right)r \quad (14)$$

Denote $A = \left(\dfrac{-6}{L^2}\omega_i + \dfrac{6}{L^2}\omega_j + \dfrac{-4}{L}\psi_i + \dfrac{-2}{L}\psi_j + \dfrac{-6}{L}\gamma_0\right)$ and $B = \left(\dfrac{12}{L^2}\omega_i + \dfrac{-12}{L^2}\omega_j + \dfrac{6}{L}\psi_i + \dfrac{6}{L}\psi_j + \dfrac{12}{L}\gamma_0\right)$

Bending energy $U_B = \dfrac{Et^3 L}{12\ 2}\displaystyle\int_0^1\left(-\frac{d\psi}{Ldr}\right)^2 dr = \dfrac{Et^3 L}{12\ 2}\displaystyle\int_0^1(A + Br)^2 dr = \dfrac{Et^3 L}{12\ 2}\left[A^2 + AB + \frac{1}{3}B^2\right]$

$$= \frac{Et^3 L}{12\ 2}\left[\left(\frac{-\psi_i}{L} + \frac{\psi_j}{L}\right)^2 + \frac{1}{12}\left(\frac{12}{L^2}\omega_i + \frac{-12}{L^2}\omega_j + \frac{6}{L}\psi_i + \frac{6}{L}\psi_j + \frac{12}{L}\gamma_0\right)^2\right] \quad (15)$$

where t is the sectional depth of the beam. Shear energy U_S per unit width of the beam is

$$U_S = \int_0^L \frac{S^2}{2GA_r}dx = \frac{GA_r L}{2}\int_0^1\left(\frac{S}{GA_r}\right)^2 dr = \frac{E5tL}{2 \times 2(1 + \mu) \times 6}\int_0^1 \gamma_0^2 dr = \frac{5EtL}{24(1 + \mu)}\gamma_0^2 \quad (16)$$

where μ is the Poisson's ratio. In Eq. (16), the effective area A_r used for shear energy determination is taken as 5/6 of the actual sectional area because of the parabolic shear stress distribution across the section. Total strain energy U is given by

$$U = U_B + U_S \quad (17)$$

The total energy is dependent on the deflection, rotation and the shear deformation and the equilibrium point is obtained by minimizing the total energy with respect to all these dependent parameters. In the present formulation, the minimum energy principle with respect to the shear deformation $\partial U/\partial\gamma_0 = 0$ is applied in addition to those for vertical deflection and rotation. By performing partial differentiation on Eq. (17) $\partial U/\partial\gamma_0 = \partial U_B/\partial\gamma_0 + \partial U_S/\partial\gamma_0 = 0$ with substitution of U_B and U_S from Eqs. (15) and (16) gives

$$\frac{\partial}{\partial\gamma_0}\left\{\frac{Et^3 L}{12\ 2}\left[\left(\frac{-\psi_i}{L} + \frac{\psi_j}{L}\right)^2 + \frac{1}{12}\left(\frac{12}{L^2}\omega_i + \frac{-12}{L^2}\omega_j + \frac{6}{L}\psi_i + \frac{6}{L}\psi_j + \frac{12}{L}\gamma_0\right)^2\right]\right\}$$

$$+ \frac{\partial}{\partial\gamma_0}\left\{\frac{5EtL}{24(1 + \mu)}\gamma_0^2\right\} = 0 \quad (18)$$

Simplifying and re-arranging

$$\gamma_0\left[\frac{5L^2 + 12(1 + \mu)t^2}{6t^2(1 + \mu)}\right] = \left[\frac{-2}{L}(\omega_i - \omega_j) - (\psi_i + \psi_j)\right] \quad (19)$$

Denote
$$\delta = \frac{6t^2(1 + \mu)}{5L^2 + 12(1 + \mu)t^2} \quad (20)$$

Eq. (19) is now re-written as

$$\gamma_0 = \frac{-2\delta}{L}\omega_i + \frac{2\delta}{L}\omega_j - \delta\psi_i - \delta\psi_j \quad (21)$$

Let the displacement vector of the shear deformable beam be represented by the vector $[\omega_i\ \psi_i\ \omega_j\ \psi_j]^T$. From Eq. (21), the strain displacement B_S matrix for the shear force is obviously given by

$$B_S = \left[\frac{-2\delta}{L}\ \ -\delta\ \ \frac{2\delta}{L}\ \ -\delta\right] \tag{22}$$

Substituting Eq. (21) into Eq. (14), we get

$$-\frac{d\psi}{L\,dr} = \frac{6(1-2r)(1-2\delta)}{L^2}\omega_i + \frac{-6(1-2r)(1-2\delta)}{L^2}\omega_j + \frac{1+3(1-2\delta)(1-2r)}{L}\psi_i$$
$$+ \frac{-1+3(1-2r)(1-2\delta)}{L}\psi_j \tag{23}$$

From Eq. (23), the strain displacement B_B matrix for the bending is given by

$$B_B = \left[\frac{6(1-2r)(1-2\delta)}{L^2}\ \ \frac{1+3(1-2\delta)(1-2r)}{L}\ \ \frac{-6(1-2r)(1-2\delta)}{L^2}\frac{-1+3(1-2\delta)(1-2r)}{L}\right] \tag{24}$$

The stiffness matrix for the shear strain is $K_s = \int_0^1 B_S^T GA_r B_S \cdot L \cdot dr$ (25)

where $GA_r = \frac{E}{2(1+\mu)}\frac{5}{6}bt = \frac{5Ebt}{12(1+\mu)}$ and B_S is from Eq. (22)

Expanding and integrating Eq. (25) gives the shear stiffness matrix as

$$K_s = \frac{5Ebt}{12(1+\mu)}\begin{bmatrix} \dfrac{4\delta^2}{L} & 2\delta^2 & -\dfrac{4\delta^2}{L} & 2\delta^2 \\[2mm] 2\delta^2 & L\delta^2 & -2\delta^2 & L\delta^2 \\[2mm] -\dfrac{4\delta^2}{L} & -2\delta^2 & \dfrac{4\delta^2}{L} & -2\delta^2 \\[2mm] 2\delta^2 & L\delta^2 & -2\delta^2 & L\delta^2 \end{bmatrix} \tag{26}$$

Similarly, the stiffness matrix for the bending is given as follows, with B_b from Eq. (24)

$$K_b = \int_0^1 B_b^T EI \cdot B_b \cdot L \cdot dr \tag{27}$$

Expanding and integrating gives the bending stiffness matrix as

$$K_b = EI\begin{bmatrix} \dfrac{12}{L^3}(1-2\delta)^2 & \dfrac{6}{L^2}(1-2\delta)^2 & -\dfrac{12}{L^3}(1-2\delta)^2 & \dfrac{6}{L^2}(1-2\delta)^2 \\[3mm] \dfrac{6}{L^2}(1-2\delta)^2 & \dfrac{4}{L}(1-3\delta+3\delta^2) & -\dfrac{6}{L^2}(1-2\delta)^2 & \dfrac{2}{L}(1-6\delta+6\delta^2) \\[3mm] -\dfrac{12}{L^3}(1-2\delta)^2 & -\dfrac{6}{L^2}(1-2\delta)^2 & \dfrac{12}{L^3}(1-2\delta)^2 & -\dfrac{6}{L^2}(1-2\delta)^2 \\[3mm] \dfrac{6}{L^2}(1-2\delta)^2 & \dfrac{2}{L}(1-6\delta+6\delta^2) & -\dfrac{6}{L^2}(1-2\delta)^2 & \dfrac{4}{L}(1-3\delta+3\delta^2) \end{bmatrix} \tag{28}$$

where $I = bt^3/12$. If thickness of the beam tends to 0 so that δ tends to 0, K_s will tends to 0 while K_b will tends to the classical beam deflection stiffness matrix. The results as given by Eqs. (26) and (28) are hence free from shear locking phenomenon. The total stiffness of the shear deformable beam is

$$K = K_s + K_b \tag{29}$$

At $r = 1/2$, substituting Eq. (21) into Eq. (12) and simplifying

$$\psi_{r=\frac{1}{2}} = \frac{-3(1-2\delta)}{2L}\omega_i + \frac{3(1-2\delta)}{2L}\omega_j + \left(-\frac{1}{4}+\frac{3}{2}\delta\right)\psi_i + \left(-\frac{1}{4}+\frac{3}{2}\delta\right)\psi_j \tag{30}$$

Eq. (30) will be used in the formulation of the pseudo 8 node thick plate element in the following section.

3. Formulation of a rectangular shear deformable plate

The foregoing derivation for shear deformable beam is extended to the formulation of rectangular plate in this section and the formulation is basically similar to the three-node Mindlin plate by Tessler and Hughes (1985). The authors have however adopted a pseudo 8 node element formulation to increase the accuracy of the element so that a good accuracy can be achieved even for a coarse mesh. Consider a rectangular plate of corner nodes 1, 2, 3, 4 and side lengths $2a$ and $2b$ as indicated in Fig. 2. Fictitious mid-side nodes 5, 6, 7 and 8 are added in the formulation but they will be statically eliminated so that only the corner nodes will be retained in the final stiffness matrix formulation. This approach is adopted as a 4 nodes element possesses good numerical accuracy but is more convenient to be used as compared with an 8 nodes element. Actually, most of the commonly used thick plate elements in various commercial programs are four nodes element (excluding those for research purpose). The 6 nodes triangular element by Sheikh and Dey (2001) is accurate but is less satisfactory for practical use because of the presence of the mid-side nodes. Any point load applied directly on the mid-side nodes will create numerical problem which is not satisfactory for practical problems.

For the plate as shown, the nodal displacement a^e of the corner nodes are given as

$$a^e = [\omega_1 \quad \psi_{x1} \quad \psi_{y1} \quad \omega_2 \quad \psi_{x2} \quad \psi_{y2} \quad \omega_3 \quad \psi_{x3} \quad \psi_{y3} \quad \omega_4 \quad \psi_{x4} \quad \psi_{y4}]^T \tag{31}$$

From Eq. (21), the shear strains at the edges $\overline{12}, \overline{23}, \overline{34}, \overline{41}$ of the element are

$$\gamma_{s12} = -\frac{\delta_a}{a}\omega_1 + \frac{\delta_a}{a}\omega_2 + \delta_a\psi_{y1} + \delta_a\psi_{y2} ; \quad \gamma_{s23} = -\frac{\delta_b}{b}\omega_2 + \frac{\delta_b}{b}\omega_3 - \delta_b\psi_{x2} - \delta_b\psi_{x3}$$

$$\gamma_{s34} = -\frac{\delta_{12}}{a}\omega_4 + \frac{\delta_{12}}{a}\omega_3 + \delta_a\psi_{y4} + \delta_a\psi_{y3} ; \quad \gamma_{s41} = -\frac{\delta_b}{b}\omega_1 + \frac{\delta_b}{b}\omega_4 - \delta_b\psi_{y1} - \delta_b\psi_{y4} \tag{32}$$

(taking note that the rotations ψ_{y1} and ψ_{y2} are clockwise positive when viewed at edge $\overline{12}, \overline{34}$ instead of anticlockwise as derived in Eq. (21))

where
$$\delta_a = \frac{\left(\frac{t}{2a}\right)^2(1+\mu)}{\frac{5}{6}+2\left(\frac{t}{2a}\right)^2(1+\mu)} = \frac{3t^2(1+\mu)}{10a^2+6t^2(1+\mu)}; \quad \delta_b = \frac{3t^2(1+\mu)}{10b^2+6t^2(1+\mu)} \tag{33}$$

t = thickness of the plate, μ = Poisson's ratio

It can easily be seen that when $t{\to}0$, δ_a, $\delta_b{\to}0$, and $\gamma_{si}{\to}0$.

The shear strain $\gamma = [\gamma_x \quad \gamma_y]^T$ within an element can be expressed as

$$\gamma_x = \sum \gamma_{xi}N_i^0 \quad \gamma_y = \sum \gamma_{yi}N_i^0 \tag{34}$$

and N_i^0 (i = 1, 2, 3, 4) are the classical bilinear interpolation functions for Q4 quadrilateral element. Substituting Eq. (32) into Eq. (34) and simplifying

$$\gamma_x = \frac{-(1-\eta)\delta_a}{2a}\omega_1 + \frac{(1-\eta)\delta_a}{2}\psi_{y1} + \frac{(1-\eta)\delta_a}{2a}\omega_2 + \frac{(1-\eta)\delta_a}{2}\psi_{y2}$$
$$+ \frac{(1+\eta)\delta_a}{2a}\omega_3 + \frac{(1+\eta)\delta_a}{2}\psi_{y3} + \frac{-(1+\eta)\delta_a}{2a}\omega_4 + \frac{(1+\eta)\delta_a}{2}\psi_{y4} \tag{35}$$

$$\gamma_y = \frac{-(1-\xi)\delta_b}{2b}\omega_1 + \frac{-(1-\xi)\delta_b}{2}\psi_{x1} + \frac{-(1+\xi)\delta_b}{2}\omega_2 + \frac{-(1+\xi)\delta_b}{2}\psi_{x2}$$
$$+ \frac{(1+\xi)\delta_b}{2b}\omega_3 + \frac{-(1+\xi)\delta_b}{2}\psi_{x3} + \frac{(1-\xi)\delta_b}{2b}\omega_4 + \frac{-(1-\xi)\delta_b}{2}\psi_{x4} \tag{36}$$

So the *B* matrix for shear is given by $\gamma = B_S a^e$ and $B_S = [B_{S1} \quad B_{S2}]$, where

$$B_{S1} = \begin{bmatrix} \frac{-(1-\eta)\delta_a}{2a} & 0 & \frac{(1-\eta)\delta_a}{2} & \frac{(1-\eta)\delta_a}{2a} & 0 & \frac{(1-\eta)\delta_a}{2} \\ \frac{-(1-\xi)\delta_b}{2b} & \frac{-(1-\xi)\delta_b}{2} & 0 & \frac{-(1+\xi)\delta_b}{2a} & \frac{-(1+\xi)\delta_b}{2} & 0 \end{bmatrix}$$

$$B_{S2} = \begin{bmatrix} \frac{(1+\eta)\delta_a}{2a} & 0 & \frac{(1+\eta)\delta_a}{2} & \frac{-(1+\eta)\delta_a}{2a} & 0 & \frac{(1+\eta)\delta_a}{2} \\ \frac{(1+\xi)\delta_b}{2b} & \frac{-(1+\xi)\delta_b}{2} & 0 & \frac{(1-\xi)\delta_b}{2b} & \frac{-(1-\xi)\delta_b}{2} & 0 \end{bmatrix} \tag{37}$$

The *D* matrix for shear is

$$D_S = G \cdot \frac{5}{6}t \cdot \begin{bmatrix} 1 & 0 \\ 0 & 1 \end{bmatrix} = \frac{E}{2(1+\mu)}\left(\frac{5t}{6}\right)\begin{bmatrix} 1 & 0 \\ 0 & 1 \end{bmatrix} = \frac{5Et}{12(1+\mu)}\begin{bmatrix} 1 & 0 \\ 0 & 1 \end{bmatrix} \tag{38}$$

The stiffness matrix for shear is given as

$$K_s^e = \int_{-b}^{b}\int_{-a}^{a}B_s^T D_S B \cdot dxdy = ab\int_{-1}^{1}\int_{-1}^{1}B_s^T D_S B \cdot d\xi d\eta \tag{39}$$
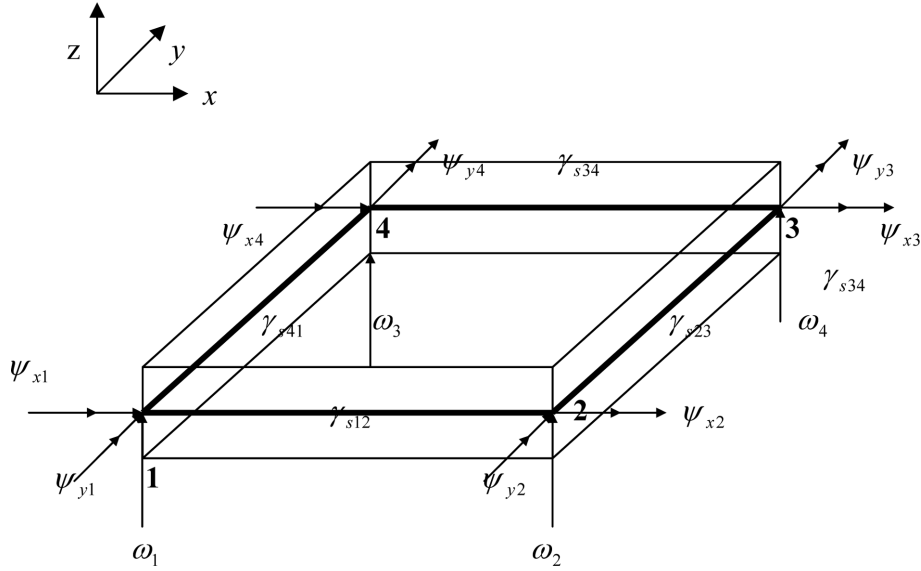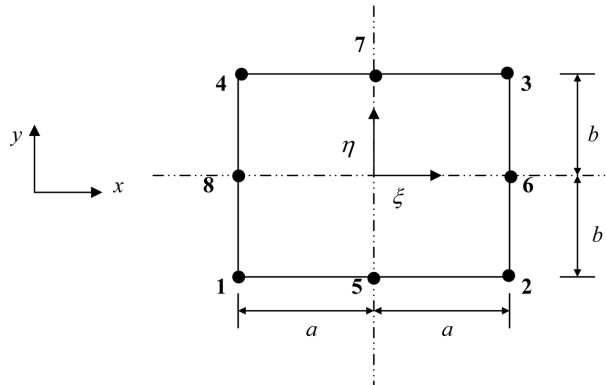
Fig. 3(a) Degree of freedom for thick plate

Fig. 3(b) Pseudo 8 node thick plate element

In the formulation of the bending stiffness matrix, normal (in the vertical plane perpendicular to the edge) and tangential rotations (in the vertical plane containing the edge) at the mid-sides nodes 5, 6, 7, 8 at the 4 edges as shown in Fig. 3(b) are first determined. For the rotations about axes parallel to the sides where these nodes are situated, the rotations are taken as average of the end nodes 1, 2, 3 and 4 for the present bilinear element as

$$\psi_{x5} = \frac{1}{2}[\psi_{x1} + \psi_{x2}]; \quad \psi_{y6} = \frac{1}{2}[\psi_{y2} + \psi_{y3}]; \quad \psi_{x7} = \frac{1}{2}[\psi_{x3} + \psi_{x4}]; \quad \psi_{y8} = \frac{1}{2}[\psi_{y1} + \psi_{y4}] \quad (40)$$

For rotations about axes perpendicular to the sides, they are determined by Eq. (30) as

$$
\left\{
\begin{aligned}
\psi_{y5} &= \frac{3(1-2\delta_a)}{4a}\omega_1 - \frac{3(1-2\delta_a)}{4a}\omega_2 + \left(-\frac{1}{4}+\frac{3}{2}\delta_a\right)\psi_{y1} + \left(-\frac{1}{4}+\frac{3}{2}\delta_a\right)\psi_{y2} \\
\psi_{x6} &= \frac{3(1-2\delta_b)}{4b}\omega_2 + \frac{3(1-2\delta_b)}{4b}\omega_3 + \left(-\frac{1}{4}+\frac{3}{2}\delta_b\right)\psi_{x2} + \left(-\frac{1}{4}+\frac{3}{2}\delta_b\right)\psi_{x3} \\
\psi_{y7} &= \frac{3(1-2\delta_a)}{4a}\omega_4 - \frac{3(1-2\delta_a)}{4a}\omega_3 + \left(-\frac{1}{4}+\frac{3}{2}\delta_a\right)\psi_{y3} + \left(-\frac{1}{4}+\frac{3}{2}\delta_a\right)\psi_{y4} \\
\psi_{x8} &= \frac{3(1-2\delta_b)}{4b}\omega_1 + \frac{3(1-2\delta_b)}{4b}\omega_4 + \left(-\frac{1}{4}+\frac{3}{2}\delta_b\right)\psi_{x1} + \left(-\frac{1}{4}+\frac{3}{2}\delta_b\right)\psi_{x4}
\end{aligned}
\right. \tag{41}
$$

The bending energy for the pseudo 8 node element is determined by the classical Q8 element shape functions as

$$
\psi_x = \sum_{i=1}^{8} N_i \psi_{xi}; \qquad \psi_y = \sum_{i=1}^{8} N_i \psi_{yi} \tag{42}
$$

Eliminating ψ_{x5} to ψ_{x8} and ψ_{y5} to ψ_{y8} by Eq. (41), so that Eq. (42) become

$$
\psi_x = -\frac{3(1-2\delta_b)}{4b}N_8\omega_1 + \left[N_1 + \frac{1}{2}N_5 + \left(-\frac{1}{4}+\frac{3}{2}\delta_b\right)N_8\right]\psi_{x1} - \frac{3(1-2\delta_b)}{4b}N_6\omega_2
$$
$$
+ \left[N_2 + \frac{1}{2}N_5 + \left(-\frac{1}{4}+\frac{3}{2}\delta_b\right)N_6\right]\psi_{x2} + \frac{3(1-2\delta_b)}{4b}N_6\omega_3 + \left[N_3 + \frac{1}{2}N_7 + \left(-\frac{1}{4}+\frac{3}{2}\delta_b\right)N_6\right]\psi_{x3}
$$
$$
+ \frac{3(1-2\delta_b)}{4b}N_8\omega_4 + \left[N_4 + \frac{1}{2}N_7 + \left(-\frac{1}{4}+\frac{3}{2}\delta_b\right)N_8\right]\psi_{x4} \tag{43}
$$

$$
\psi_y = \frac{3(1-2\delta_a)}{4a}N_5\omega_1 + \left[N_1 + \frac{1}{2}N_8 + \left(-\frac{1}{4}+\frac{3}{2}\delta_a\right)N_5\right]\psi_{y1} - \frac{3(1-2\delta_a)}{4a}N_5\omega_2
$$
$$
+ \left[N_2 + \frac{1}{2}N_6 + \left(-\frac{1}{4}+\frac{3}{2}\delta_a\right)N_5\right]\psi_{y2} - \frac{3(1-2\delta_a)}{4a}N_7\omega_3 + \left[N_3 + \frac{1}{2}N_6 + \left(-\frac{1}{4}+\frac{3}{2}\delta_a\right)N_7\right]\psi_{y3}
$$
$$
+ \frac{3(1-2\delta_a)}{4a}N_7\omega_4 + \left[N_4 + \frac{1}{2}N_8 + \left(-\frac{1}{4}+\frac{3}{2}\delta_a\right)N_7\right]\psi_{y4} \tag{44}
$$

The 4 node element formulation as proposed is hence a pseudo 8 node formulation which will increase the accuracy of the solution. It should be pointed out that different order are used for bending and shear energy terms which is better than the classical Q8 Mindlin plate element formulation (Zienkiewicz 1991).

The curvature matrix of the plate element is given by

$$
\kappa = \begin{pmatrix} \kappa_x & \kappa_y & \kappa_{xy} \end{pmatrix}^T = \left(\frac{\partial\psi_x}{\partial y} \quad \frac{\partial\psi_y}{\partial x} \quad \frac{\partial\psi_y}{\partial y} - \frac{\partial\psi_x}{\partial x} \right)^T \tag{45}
$$

Using

$$
\frac{\partial\psi_x}{\partial y} = \frac{\partial\psi_x}{\partial\eta}\cdot\frac{\partial\eta}{\partial y} = \frac{\partial\psi_x}{\partial\eta}\cdot\frac{1}{b}; \qquad \frac{\partial\psi_y}{\partial x} = \frac{\partial\psi_y}{\partial\xi}\cdot\frac{\partial\xi}{\partial x} = \frac{\partial\psi_y}{\partial\xi}\cdot\frac{1}{a}
$$

$$\frac{\partial \psi_y}{\partial y} = \frac{\partial \psi_y}{\partial \eta} \cdot \frac{\partial \eta}{\partial y} = \frac{\partial \psi_y}{\partial \eta} \cdot \frac{1}{b}; \quad \frac{\partial \psi_x}{\partial x} = \frac{\partial \psi_x}{\partial \xi} \cdot \frac{\partial \xi}{\partial x} = \frac{\partial \psi_x}{\partial \xi} \cdot \frac{1}{a} \tag{46}$$

By appropriately differentiating Eqs. (43) and (44), the B matrix for bending as equated by $\kappa = B_B a^e$ would be $B_B = [B_{B1} \ B_{B2} \ B_{B3} \ B_{B4}]$, where

$$B_{B1} = \begin{bmatrix} \dfrac{3(1-2\delta_b)(1-\xi)\eta}{4b^2} & \dfrac{(1-\xi)(3\eta-1-6\eta\delta_b)}{4b} & 0 \\[2em] -\dfrac{3(1-2\delta_a)(1-\eta)\xi}{4a^2} & 0 & \dfrac{(1-\eta)(3\xi-1-6\delta_a\xi)}{4a} \\[2em] \dfrac{3[(1-2\delta_a)(1-\xi^2)+(1-2\delta_b)(1-\eta^2)]}{-8ab} & \dfrac{(1-\eta)[-3\eta-1+6\delta_b(1+\eta)]}{8a} & \dfrac{(1-\xi)[3\xi+1-6\delta_a(1+\xi)]}{8b} \end{bmatrix} \tag{47}$$

The other B matrices are similar to Eq. (47) and will not be given here. The D_b matrix for bending is given by $[M_x \ M_y \ M_{xy}]^T = D_b \kappa$ as

$$D_b \begin{Bmatrix} \dfrac{\partial \psi_x}{\partial y} \\[1em] \dfrac{\partial \psi_y}{\partial x} \\[1em] \left(\dfrac{\partial \psi_x}{\partial x} - \dfrac{\partial \psi_y}{\partial y}\right) \end{Bmatrix}; \quad D_b = \frac{Et^3}{12(1-\mu^2)} \begin{bmatrix} 1 & -\mu & 0 \\ -\mu & 1 & 0 \\ 0 & 0 & \dfrac{1-\mu}{2} \end{bmatrix} \tag{48}$$

So, the stiffness matrix for bending can be formed by expanding and integrating the following expression

$$K_b^e = \int_{-b}^{b}\int_{-a}^{a} B_B^T D_b B_B \, dx \, dy = ab \int_{-1}^{1}\int_{-1}^{1} B_B^T D_b B_B \, d\xi \, d\eta \tag{49}$$

The total stiffness of the plate element will be $K = K_s^e + K_b^e$ \hfill (50)

4. Extension of "PLATE" to general quadrilateral element

With minor changes to the formulation (but more complicated equations), the rectangular thick "PLATE" element as given in previous section can be extended to a general quadrilateral element as follows. From Eq. (32), the shear strains at the edge ij of a general quadrilateral element is

$$\gamma_{sij} = -\frac{\delta_{ij}}{l_{ij}}[2(\omega_i - \omega_j) + (\psi_i + \psi_j)l_{ij}]$$

$$= -\frac{\delta_{ij}}{l_{ij}}[2(\omega_i - \omega_j) + \psi_{xi}\Delta y_{ji} - \psi_{yi}\Delta x_{ji} + \psi_{xj}\Delta y_{ji} - \psi_{yj}\Delta x_{ji}] \tag{51}$$

where, $\Delta x_{ji} = x_j - x_i$, $\Delta y_{ji} = y_j - y_i$ \hfill (52)

$$\delta_{ij} = \frac{\left(\dfrac{t}{l_{ij}}\right)^2 (1+\mu)}{\dfrac{5}{6} + 2\left(\dfrac{t}{l_{ij}}\right)^2 (1+\mu)} \qquad (i,j = 1,2,3,4) \tag{53}$$

For convenience, a term γ^*_{sij} is defined and is given $\gamma^*_{sij} = l_{ij}\gamma_{rij}$ $(i = 1,2,3,4)$

$$\gamma^*_s = \begin{bmatrix} \gamma^*_{s12} & \gamma^*_{s23} & \gamma^*_{s34} & \gamma^*_{s41} \end{bmatrix}^T \tag{54}$$

then

$$\gamma^*_s = T_s a^e \tag{55}$$

$$T_s = \begin{bmatrix} -2\delta_{12} & -\delta_{12}\Delta y_{21} & \delta_{12}\Delta x_{21} & 2\delta_{12} & -\delta_{12}\Delta y_{21} & \delta_{12}\Delta x_{21} & 0 & 0 & 0 & 0 & 0 & 0 \\ 0 & 0 & 0 & -2\delta_{23} & -\delta_{23}\Delta y_{32} & \delta_{23}\Delta x_{32} & 2\delta_{23} & -\delta_{23}\Delta y_{32} & \delta_{23}\Delta x_{32} & 0 & 0 & 0 \\ 0 & 0 & 0 & 0 & 0 & 0 & -2\delta_{34} & -\delta_{34}\Delta y_{43} & \delta_{34}\Delta x_{43} & 2\delta_{34} & -\delta_{34}\Delta y_{43} & \delta_{34}\Delta x_{43} \\ 2\delta_{41} & -\delta_{41}\Delta y_{14} & \delta_{41}\Delta x_{14} & 0 & 0 & 0 & 0 & 0 & 0 & -\delta_{41} & -\delta_{41}\Delta y_{14} & \delta_{41}\Delta x_{14} \end{bmatrix} \tag{56}$$

As the axes are not along the main directions, transformation of strain from local to global axes will be required, and the nodal shear strain will become

$$\begin{Bmatrix} \gamma_{xi} \\ \gamma_{yi} \end{Bmatrix} = \frac{1}{\Delta y_{ik}\Delta x_{ji} - \Delta y_{ji}\Delta x_{ik}} \begin{bmatrix} \Delta y_{ik} & -\Delta y_{ji} \\ -\Delta x_{ik} & \Delta x_{ji} \end{bmatrix} \begin{Bmatrix} r^*_{sij} \\ r^*_{ski} \end{Bmatrix} \tag{57}$$

$$= \begin{bmatrix} T_{sx} \\ T_{sy} \end{bmatrix} \begin{Bmatrix} r^*_{sij} \\ r^*_{ski} \end{Bmatrix}$$

where $j = i+1$ if $j < 5$ and $= 1$ if $j = 5$; $k = i-1$ if $k > 1$ else $k = 4$. The nodal shear strain can be expressed in terms of the nodal displacement as

$$\begin{rcases} \gamma_{xi} = T_{sx}\gamma^*_s = T_{sx}T_s a^e \\ \gamma_{yi} = T_{sy}\gamma^*_s = T_{sy}T_s a^e \end{rcases} \tag{58}$$

or

$$\gamma_{xi} = \begin{bmatrix} \gamma_{x1} & \gamma_{x2} & \gamma_{x3} & \gamma_{x4} \end{bmatrix}^T, \quad \gamma_{yi} = \begin{bmatrix} \gamma_{y1} & \gamma_{y2} & \gamma_{y3} & \gamma_{y4} \end{bmatrix}^T$$

Eqs. (35) and (36) will become

$$\gamma = \begin{Bmatrix} \gamma_x \\ \gamma_y \end{Bmatrix} = \begin{bmatrix} N_s T_{sx} T_s \\ N_s T_{sy} T_s \end{bmatrix} a^e = B_s a^e \tag{59}$$

where

$$B_S = \begin{bmatrix} N_s T_{sx} T_s \\ N_s T_{sy} T_s \end{bmatrix} \tag{60}$$

and the shape function matrix N is given by $N = \begin{bmatrix} N_1 & N_2 & N_3 & N_4 \end{bmatrix}$ \tag{61}

Shear stiffness for this general quadrilateral element will still be given by Eq. (39) but B_s as given

by Eq. (60) will be used.

The normal rotation ψ_n and tangential rotation ψ_s for the mid-side nodes can be expressed as

$$\psi_{nij} = \psi_{xij}\cos\theta_{ij} + \psi_{yij}\sin\theta_{ij} \qquad \psi_{sij} = \psi_{xij}\sin\theta_{ij} - \psi_{yij}\cos\theta_{ij} \tag{62}$$

where θ_{ij} is the angle of the line $\overline{ij}$ with the *X*-axis.

$$\Rightarrow \psi_{nij} = \psi_{xij}\frac{x_j - x_i}{l_{ij}} + \psi_{yij}\frac{y_j - y_i}{l_{ij}} = \psi_{xij}\frac{\Delta x_{ji}}{l_{ij}} + \psi_{yij}\frac{\Delta y_{ji}}{l_{ij}} \tag{63}$$

$$\Rightarrow \psi_{sij} = \psi_{xij}\frac{y_j - y_i}{l_{ij}} - \psi_{yij}\frac{x_j - x_i}{l_{ij}} = \psi_{xij}\frac{\Delta y_{ji}}{l_{ij}} - \psi_{yij}\frac{\Delta x_{ji}}{l_{ij}} \tag{64}$$

$$\text{or} \quad \begin{Bmatrix} \psi_{nij} \\ \psi_{sij} \end{Bmatrix} = \frac{1}{l_{ij}}\begin{bmatrix} \Delta x_{ji} & \Delta y_{ji} \\ \Delta y_{ji} & -\Delta x_{ji} \end{bmatrix}\begin{Bmatrix} \psi_{xij} \\ \psi_{yij} \end{Bmatrix} \tag{65}$$

For node 5, the normal shear strain is

$$\psi_{n5} = \frac{1}{2}[(\psi_{n1})_{\overline{12}} + (\psi_{n2})_{\overline{12}}] = \frac{1}{2l_{12}}[\Delta x_{21}(\psi_{x1} + \psi_{x2}) + \Delta y_{21}(\psi_{y1} + \psi_{y2})] \tag{66}$$

Similar equations can be written for nodes 6, 7, 8 and will not be repeated here. According to Eq. (12), the tangential rotations at mid-side nodes 5, 6, 7, 8 are

$$\psi_{s5} = \frac{1}{2}\psi_{s1} + \frac{1}{2}\psi_{s2} + 3(1 - 2\delta_{12})\left[\frac{2}{l_{12}}(-\omega_1 + \omega_2) - \psi_{s1} - \psi_{s2}\right]\frac{1}{4}$$

$$= \frac{3}{2l_{12}}(1 - 2\delta_{12})(\omega_2 - \omega_1) - \frac{1}{4l_{12}}(1 - 6\delta_{12})[\Delta y_{21}(\psi_{x1} + \psi_{x2}) - \Delta x_{21}(\psi_{y1} + \psi_{y2})] \tag{67}$$

Similar equations can also be established for nodes 6,7 and 8 and will not be repeated here. For rotation at mid-side nodes, inverting Eq. (67) for node 5

$$\begin{Bmatrix} \psi_{x5} \\ \psi_{y5} \end{Bmatrix} = \frac{1}{l_{12}}\begin{bmatrix} \Delta x_{21} & \Delta y_{21} \\ \Delta y_{21} & -\Delta x_{21} \end{bmatrix}\begin{Bmatrix} \psi_{n5} \\ \psi_{s5} \end{Bmatrix} \tag{68}$$

$$\psi_{x5} = \frac{1}{l_{12}}(\Delta x_{21}\psi_{n5} + \Delta y_{21}\psi_{s5}) \tag{69}$$

$$= -\frac{3\Delta y_{21}}{2l_{12}^2}(1 - 2\delta_{12})\omega_1 + \frac{1}{2l_{12}^2}\left[\Delta x_{21}^2 - \frac{\Delta y_{21}^2}{2}(1 - 6\delta_{12})\right]\psi_{x1} + \frac{\Delta x_{21}\Delta y_{21}}{2l_{12}^2}\left[1 + \frac{1}{2}(1 - 6\delta_{12})\right]\psi_{y1}$$

$$+ \frac{3\Delta y_{21}}{2l_{12}^2}(1 - 2\delta_{12})\omega_2 + \frac{1}{2l_{12}^2}\left[\Delta x_{21}^2 - \frac{\Delta y_{21}^2}{2}(1 - 6\delta_{12})\right]\psi_{x2} + \frac{\Delta x_{21}\Delta y_{21}}{2l_{12}^2}\left[1 + \frac{1}{2}(1 - 6\delta_{12})\right]\psi_{y2} \tag{70}$$

$$\psi_{y5} = \frac{1}{l_{12}}(\Delta y_{21}\psi_{n5} - \Delta x_{21}\psi_{s5}) \tag{71}$$

$$= \frac{3\Delta x_{21}}{2l_{12}^2}(1 - 2\delta_{12})\omega_1 + \frac{\Delta x_{21}\Delta y_{21}}{2l_{12}^2}\left[1 + \frac{1}{2}(1 - 6\delta_{12})\right]\psi_{x1} + \frac{1}{2l_{12}^2}\left[\Delta y_{21}^2 - \frac{\Delta x_{21}^2}{2}(1 - 6\delta_{12})\right]\psi_{y1}$$

$$- \frac{3\Delta x_{21}}{2l_{12}^2}(1 - 2\delta_{12})\omega_2 + \frac{\Delta x_{21}\Delta y_{21}}{2l_{12}^2}\left[1 + \frac{1}{2}(1 - 6\delta_{12})\right]\psi_{x2} + \frac{1}{2l_{12}^2}\left[\Delta y_{21}^2 - \frac{\Delta x_{21}^2}{2}(1 - 6\delta_{12})\right]\psi_{y2} \qquad (72)$$

Similar results can be written for the other mid-side nodes which will not be repeated here. It is now possible to express the shear strain in terms of the nodal displacement within the general quadrilateral element by extending Eq. (42) with equations Eqs. (70) and (72). The authors have adopted the symbolic algebra program Mathcad for generating the resulting strain-displacement matrix B_B. The complete equations formed by the use of program Mathcad are lengthy and will not be reproduced here.

5. Problems of the IB element and the performance of the "PLATE" element

IB element is commonly used by many engineers in Hong Kong, China and many other countries. The authors have discovered two interesting problems with the use of the IB element which will be discussed here. The first case is a 1.5 m thick plate (as pile cap) supported on steel H-piles as illustrated in Fig. 4 and the rectangular IB element is used for the analysis. The plate is loaded with UDL, line loads and point loads and is analyzed for different degrees of meshing determined by the use of different maximum element sizes. For illustration purpose, M_y moment which is the bending moment along the axis parallel to grid X1 to X4 are obtained for the free edge (unsupported) of the cap between grid X3 and X4 near grid XC and is plotted in Figs. 4 and 5. This moment is considered as it should be 0 along this free edge so that comparisons will be meaningful.

Whilst M_y moment should theoretically be zero along the free edge, it can be seen from Fig. 5 that the IB element give high values of M_y for a maximum element size of 1m which is the also default value as adopted in some popular programs. M_y becomes smaller as the maximum element size reduces to 0.2 m for the IB element. This phenomenon has also illustrated a well known fact that results from finite element analysis can converge to accurate values at fine meshing.
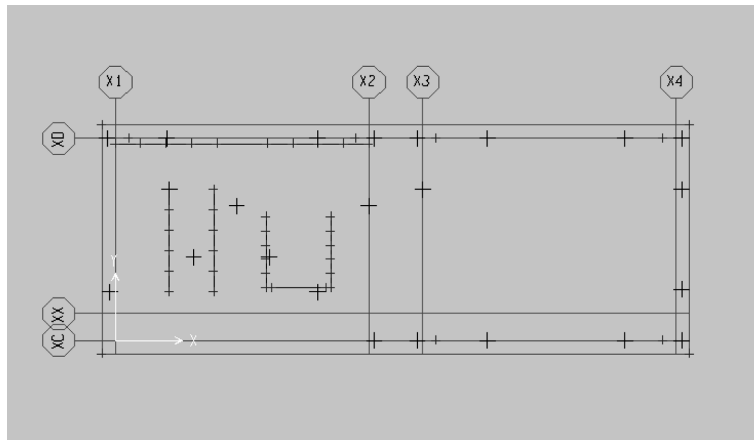

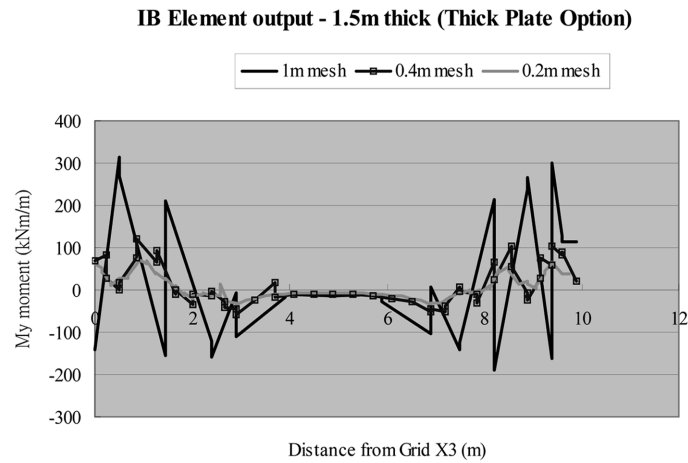Fig. 4 Moment at cantilever end for a thick plate

IB Element output - 1.5m thick (Thick Plate Option)

Fig. 5 M_y along free edge for different mesh size by IB element (plate thickness 1.5 m)

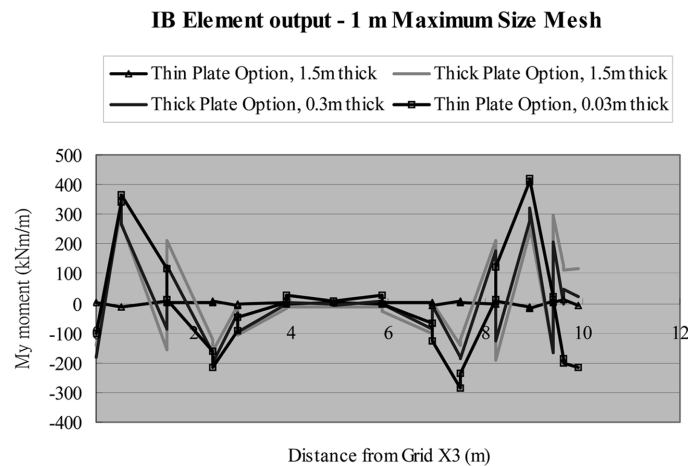**IB Element output - 1 m Maximum Size Mesh**

Fig. 6 M_y along free edge for plate thickness by IB element (maximum element size 1 m)

The structure is then re-analyzed with the IB element with a maximum element size equal to 1 m under (i) thin plate option for 1.5 m structural thickness; (ii) thick plate option of 1.5 m thickness; (iii) thick plate option of 0.3 m thickness; (iv) thick plate option of 0.03 m thickness. In Fig. 6, the "thin" plate option has yielded very small values for the M_y moments which is considered to be very accurate. However, it is surprising to note that under the option of "thick plate", M_y moments diverge to very high values when the plate thickness is reduced instead of converging to nearly zero as obtained by the thin "Kirchhoff Plate". That means, if the element size is maintained constant, results from IB element will diverge with decreasing plate thickness!

In comparison, the structure is analyzed by "PLATE" developed in the present paper with the same mesh. M_y moment are small when the plate thickness is thin as shown in Fig. 7, and this has demonstrated that "PLATE" can converge to thin plate solution without "shear locking" while the convergence of the IB element is poor showing that it actually experiences "shear locking".

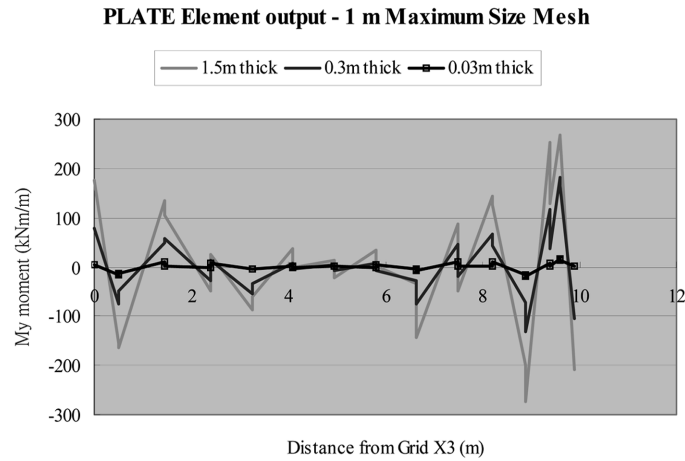**PLATE Element output - 1 m Maximum Size Mesh**

Fig. 7 M_y along free edge for different plate thickness based on present formulation (maximum element size = 1.0 m)

Ibrahimbegovic (1993) has demonstrated that IB element is free from shear locking for several different cases but has not considered the case for a cantilever edge which is now proved to exhibit "shear locking" phenomenon. The reason for this surprising phenomenon is that severe warping of the section has occurred along free edge and the minimization of shear strain energy as given by $\partial U / \partial \gamma_0 = 0$ and Eq. (19) which will reduce the over-stiff rigidity arising from the finite element discretization is absent in the IB element.

The second interesting case is a 1 unit width thin square plate supported on four stiff walls along its perimeter and a unit distributed load is applied on the square plate. The wall loading for this case will be independent of the thickness and Young's modulus of the plate. For the present problem, there are 21 rows of element along the *x*-direction and 18 rows of element along the *y*-direction in the finite element model. The structure itself is symmetric in nature while the mesh along *x* and *y* directions are not the same. For the IB thin plate element, the wall loadings along *x* and *y* directions differ by 4.8% while the corresponding difference by "PLATE" is 3%. This example illustrates that the use of the IB element is more affected by the design of the mesh as compared with the use of "PLATE".

Another interesting problem with the IB element is discovered for the raft footing foundation supported on ground in Hong Kong which is shown in Fig. 8. Assembly of the rectangular IB elements with some triangular elements at periphery of the footing is used for the analysis of this raft footing. The concrete structural thickness is 800 mm and it is supported on soil with subgrade reaction constant equal to 300 kPa/m^2. A very fine mesh has been adopted for this project so that the results are not affected by the mesh design. There are altogether 3 surprising "shear jumps" arising from the use of the IB element within the raft foundation for which the shear force varies significantly over a small distance. V_{XZ} along a line of the footing is shown in Fig. 9 and a shear jump at *x* equal to 24 m is noticed. As no point load or support is applied at these shear jump locations and these shear jump locations are not at the periphery of the footing, such shear jumps are surprising and the results are considered as reasonable. Yet this problem can easily be overlooked by the engineer as it is a common practice that the engineer uses the averaged result over a certain structural width instead of the local result for design. In comparison, the authors have
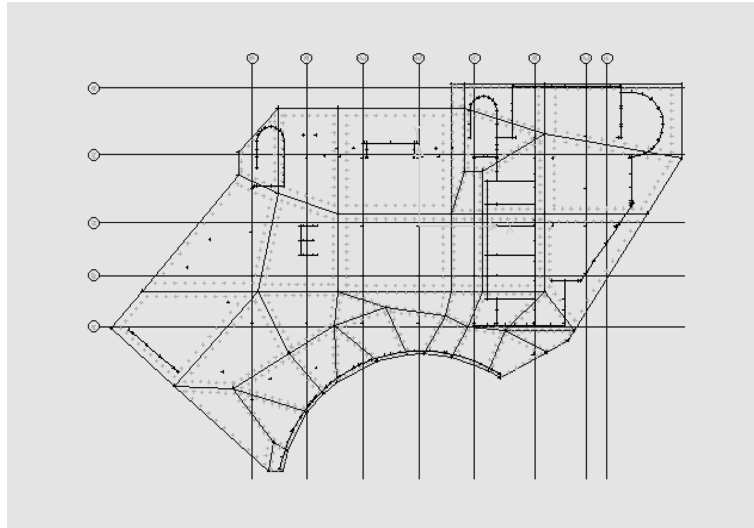
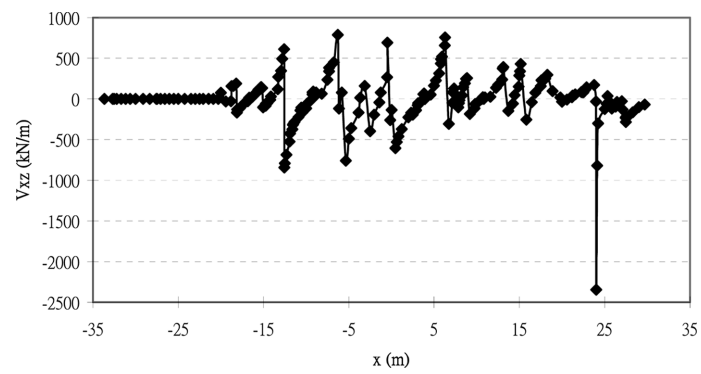Fig. 8 Shear jump for a raft footing

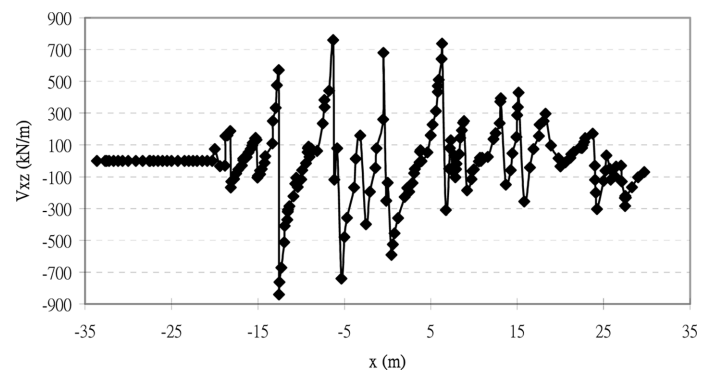Fig. 9 Shear jump at raft footing by IB element (y = 7.7 m)

Fig. 10 Raft footing analysis by "PLATE" (y = 7.7 m)

performed the same analysis by the "PLATE" (quadrilateral elements instead of rectangular elements are used in this problem) and no shear jump is found. Plot of V_{XZ} along the same strip of Fig. 9 is produced in Fig. 10, revealing no shear jump at $x = 24$ m. The reason for such a strange phenomenon arising from the use of IB element is not clear, but the authors suspect that the 'over-stiff' behaviour of the IB element as demonstrated in Fig. 6 may be one of the possible reasons behind this unreasonable phenomenon. The results of Fig. 8 and Fig. 9 are usually close with the maximum difference less than 5% except for the shear jump. Such results also illustrate that the accuracy of IB element and "PLATE" are similar when the mesh is fine.

Finally, a standard problem of a square plate simply supported on four sides with hard support condition (rotation along the support is zero) and a uniformly distributed load q is applied. Rigorous solutions given by Reismann (1988) and Sziland (2004) are used for comparison in the study. The authors have reviewed most of the thick/thin plate elements within 2000 to 2006, and some useful results from the modern elements are given in Tables 1 and 2. The maximum moment M_x and deflection ω which are at the centre of the plate are analyzed and normalized with respect to $0.01qL^2$ and qL^4/D so that the moment and deflection coefficients under different degrees of meshing can be compared.

From Tables 1 and 2, it is noticed that "PLATE" can provide very good accuracy even when the mesh is very coarse, which is not easily achieved in the finite element analysis. For the moment coefficients, they are slightly less accurate as compared with the deflection coefficients which are expected from displacement based finite element analysis. But even so, the moment coefficients are very good for a coarse mesh if the t/L ratio is less than 0.1. For a mesh size of 8×8 which is still relatively coarse, the results by the present element are very good for both the moment and deflection. The results are even better for further finer meshes. On the other hand, the performance of the popular IB element is relatively poor for both the deflection and moment with a coarse mesh. For a mesh size of 32×32 which is relatively fine, the accuracy of the IB element is fair for the deflection but is still relatively poor for the moment unless the thickness of the plate is small. In conclusion, the performance of the popular IB element is not good enough and the rate of convergence of the results with increasing number of elements is only fair. Plate is also slightly more accurate than RDKQM and DKTM/RDKTM. Compared with ARS-Q12, the moment coefficients from PLATE is better than the ARS-Q12 when $t/l \leq 0.15$, while the reverse situation will happen when $t/l \geq 0.15$. The comparisons of the 6 node triangular element by Sheikh and Dey are similar to that for ARS-Q12. For the thickness/span ratios commonly encountered in civil engineering, "PLATE" can provide very accurate solutions with coarse meshes.

Over the past two decades, many thick plate elements have been developed (Zienkiewicz 2000). The use of bubble functions by Taylor and others which is similar to the addition of incompatible mode by Wilson (1973) is generally an effective way to increase the accuracy of solution. But physically it is less direct than the present formulation of "PLATE" where only energy minimization is used. Those elements based on the use of bubble functions (used by Taylor in program FEAP), stabilization matrix (Hughes 1987) or substitute shear strain (RDKQM, DKTM, RDKTM) are mathematically simpler than the present formulation. But the present formulation possesses the advantage of using total energy consideration without the need of artificial compensations in form of bubble functions or stabilization matrices. Even though the resulting matrices from the present formulation are more complicated in the form, the present formulation is easier to understand as compared with most of the modern thick plate formulation. Zienkiewicz and Taylor (2000) have carried out a detailed comparison between the normalized moment and deflection coefficients for

Table 1 Bending moment (M_x) coefficients at the centre of plate for different thickness/span ratios and mesh sizes ($\mu = 0.3$ and the bending moment coefficient by rigorous solution is 0.04789)

	2×2	4×4	8×8	16×16	32×32
	$t/L = 0.001$				
IB	0.03921	0.04878	0.04808	0.048	0.04798
"PLATE"	0.0487	0.04779	0.04784	0.04787	0.04788
ARS-Q12	0.05009	0.04839	0.04801	0.04792	—
	$t/L = 0.01$				
IB	0.03923	0.04892	0.04865	0.04836	0.04805
"PLATE"	0.04872	0.04781	0.04786	0.0479	0.0479
RDKQM	0.05015	0.04842	0.04804	—	—
DKTM /RDKTM	0.04779 /0.05165	0.04819 /0.04876	0.04805 /0.04818	—	—
ARS-Q12	0.05012	0.04842	0.04804	0.04794	—
Sheikh and Dey	0.0502	0.04847	0.04805	—	—
	$t/L = 0.1$				
IB	0.04079	0.05291	0.05076	0.04959	0.0493
"PLATE"	0.05061	0.04937	0.0486	0.04812	0.04795
ARS-Q12	0.05223	0.04841	0.04834	0.04801	—
Sheikh and Dey	0.05124	0.04884	0.04814	—	—
	$t/L = 0.15$				
IB	0.04242	0.0542	0.05177	0.05067	0.05037
"PLATE"	0.05249	0.05026	0.04876	0.04814	0.04795
Sheikh and Dey	0.05140	0.04886	0.04814	—	—
	$t/L = 0.2$				
IB	0.04423	0.05531	0.05288	0.05185	0.05157
"PLATE"	0.05448	0.05088	0.04884	0.04814	0.04795
RDKQM	0.05430	0.04973	0.04837	—	—
DKTM/RDKTM	0.05775/0.05556	0.05062/0.05042	0.04859/0.04858	—	—
ARS-Q12	0.05429	0.04972	0.04837	0.04801	—
Sheikh and Dey	0.05147	0.04887	0.04814	—	—
	$t/L = 0.25$				
IB	0.04601	0.05631	0.05397	0.05302	0.05276
"PLATE"	0.05634	0.05129	0.04888	0.04814	0.04795
Sheikh and Dey	0.05150	0.04888	0.04814	—	—
	$t/L = 0.3$				
IB	0.04764	0.0572	0.05497	0.05409	0.05385
"PLATE"	0.05797	0.05157	0.0489	0.04815	0.04795
ARS-Q12	0.05523	0.04981	0.04837	0.04801	—
	$t/L = 0.35$				
IB	0.04905	0.05797	0.05587	0.05505	0.05482
"PLATE"	0.05932	0.05176	0.04891	0.04815	0.04795
ARS-Q12	0.05549	0.04983	0.04838	0.04801	—

Table 2 Deflection coefficients at the centre of plate for different thickness/span ratios and mesh sizes (μ = 0.3)

|	2×2	4×4	8×8	16×16	32×32
t/L = 0.001 (coefficient = 0.004062 by rigorous solution)					
IB	0.002891	0.003724	0.003523	0.003847	0.003853
"PLATE"	0.003784	0.004045	0.004059	0.004061	0.004061
ARS-Q12	0.004045	0.004060	0.004062	0.004062	—
t/L = 0.01 (coefficient = 0.004064 by rigorous solution)					
IB	0.002895	0.003733	0.003848	0.003869	0.003892
"PLATE"	0.003787	0.004048	0.004061	0.004064	0.004064
RDKQM	0.004048	0.004062	0.004063	—	—
DKTM/RDKTM	0.003972/0.004058	0.004044/0.004069	0.004061/0.004065	—	—
ARS-Q12	0.003993	0.004046	0.004060	—	—
t/L = 0.1 (coefficient = 0.004273 by rigorous solution)					
IB	0.003307	0.004226	0.004233	0.004203	0.004194
"PLATE"	0.003997	0.004229	0.004256	0.004267	0.004272
ARS-Q12	0.004047	0.004062	0.004063	0.004064	—
Sheikh and Dey	0.004212	0.004258	0.004269	—	—
t/L = 0.15 (coefficient = 0.004536 by rigorous solution)					
IB	0.003793	0.00463	0.0046	0.004573	0.004566
"PLATE"	0.004276	0.004485	0.004518	0.004531	0.004535
Sheikh and Dey	0.004484	0.004523	0.004533	—	—
t/L = 0.2 (coefficient = 0.004906 by rigorous solution)					
IB	0.004426	0.005131	0.005081	0.005055	0.005049
"PLATE"	0.004687	0.004857	0.004888	0.004899	0.004903
RDKQM	0.004858	0.004889	0.004900	—	—
DKTM/RDKTM	0.005001/0.004902	0.004932/0.004904	0.004913/0.004906	—	—
ARS-Q12	0.004857	0.004889	0.004900	0.004903	—
Sheikh and Dey	0.004864	0.004894	0.004902	—	—
t/L = 0.25 (coefficient = 0.005379 by rigorous solution)					
IB	0.005184	0.005731	0.005664	0.005638	0.005631
"PLATE"	0.005233	0.005348	0.005369	0.005377	0.005377
Sheikh and Dey	0.005352	0.005371	0.005376	—	—
t/L = 0.3 (coefficient = 0.005956 by rigorous solution)					
IB	0.006056	0.006428	0.006342	0.006314	0.00631
"PLATE"	0.005923	0.005951	0.005953	0.005956	0.005956
ARS-Q12	0.005950	0.005953	0.005956	0.005956	—
t/L = 0.35 (coefficient = 0.006641 by rigorous solution)					
IB	0.007036	0.00722	0.007113	0.007081	0.007073
"PLATE"	0.006753	0.006678	0.006645	0.006642	0.006641
ARS-Q12	0.006667	0.006646	0.006642	0.006641	—
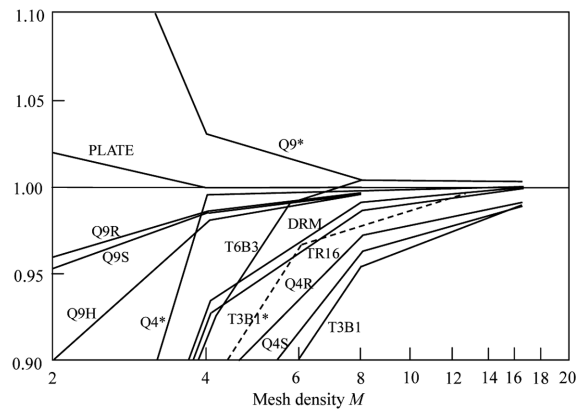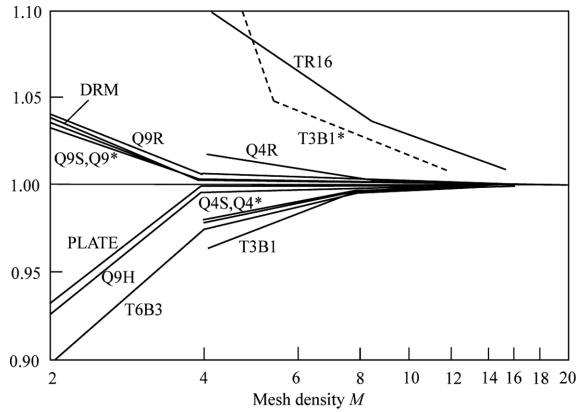
Fig. 11 Normalized displacement coefficient   Fig. 12 Normalized moment coefficient
with respect to thin plate solution for simply supported, uniformly loaded square plate ($t/l = 0.01$)

various thick plate elements and the results from "PLATE" are added to the comparisons which are shown in Figs. 11 and 12.

With reference to the results by Zienkiewicz and Taylor (2000), it is noted that the "PLATE" element has demonstrated very high accuracy and is practically the best element among those elements as shown in Figs. 11 and 12. For a mesh of 4×4, results from "PLATE" are practically exact which are not possible with all of the other thick plate elements. Interestingly, "PLATE" is more accurate than the 9 nodes elements, and this result has demonstrated that, apart from the order of the element, the formulation of the element is an important factor for the success of a good thick plate element.

Though the "PLATE" element yields very accurate results, its formulation is however more complicated than the IB element which is commonly used by many engineers. Nevertheless, once the element is programmed, it can be used in a way similar to any other classical thick plate element with only minor increase in computation efforts as most of the computer time is devoted to solution of stiffness matrix equations rather than stiffness matrix formulations. By using the Fortran compiler in developing "PLATE", the authors have compared solution time with the commercial program using the IB elements based on the same compiler. The total solution times for a mesh with 16641 nodes are virtually the same for IB element and "PLATE". For a smaller mesh, the use of "PLATE" will take only slightly longer solution time and a much better accuracy can be achieved.

6. Discussion and conclusion

In the present paper, the authors have discovered some problems with the IB element which is being used by many engineers in different countries for thick plate analysis. As demonstrated in Figs. 5 and 6, very surprising results may be obtained along the free edge where there is serious warping. The popular IB element may experience shear lock phenomenon at cantilever edge if the thickness is small and the element size is large. On the other hand, "PLATE" can perform well for cantilever edge at different plate thickness and element size.

In addition, the authors have also discovered some surprising shear jump phenomenon as shown in Fig. 8. Actually, the authors have also discovered surprising moment and twisting moment jump from the present study, but these problems are less critical compared with the shear jump phenomenon as shear force is formed by the derivative of the moment. The authors suggest that engineers should perform proper analyses and designs based on knowledge and judgment and more efforts should be spent in the analysis and detailed study of the results. In particular, besides the averaged results used for analysis, the local results should also be studied which may reveal problems. This problem has emerged but is often left unnoticed which is due to the over-reliance on the use of computer software and the averaged nodal results for design by some engineers without full awareness of these "jumps" across elements. Designers are strongly advised to check the "stresses" in the individual elements to spot if the "jumps" are significant before the average nodal results are used for design.

In view of the problems with the popular IB element, the authors have developed a new thick plate element "PLATE" which can overcome the problems of the IB element. "PLATE" has better shear strain treatment and will produce better results as compared with the IB element, especially at locations with heavy warping. The authors have studied four cases (two of which originate from real jobs in Hong Kong) and the problems of the popular IB element are clearly illustrated. "PLATE" has performed well in all these interesting cases. The formulation of "PLATE" is based on energy minimization which is more direct to engineers as compared with the use of bubble functions, substitute shear strain or stabilization matrices. Since a very high accuracy can be achieved by "PLATE", the more cumbersome efforts in forming the stiffness matrix of the element in computation can be well balanced off by the use of a coarse mesh but with greater accuracy. Compared with the recent thin/thick plate elements, the present formulation is better than those based on the substitute shear strain and are comparable to the other modern thin/thick plate elements. For most practical applications where the thickness/span ratio is less than 0.2, the present formulation provides a good solution for engineering use which is illustrated in Tables 1 and 2.

9 nodes or 8 nodes elements can provide good accuracy which can be seen from Figs. 8 and 9. They are however not convenient to be used in practice and the accuracy of "PLATE" is actually as good as those 9 nodes elements. For practical applications, most of the engineers and computer softwares adopt 4 nodes elements to suit the superstructure layout and loadings. From Fig. 11 and 12, the accuracy of "PLATE" is far better than many 4 nodes elements and the present thick plate element can be useful to large transfer plate where a fine mesh can be very time consuming in analysis.

References

Abdalla, J.A. and Ibrahim, A.K. (2007), "A geometrically nonlinear thick plate bending element based on mixed formulation and discrete collocation constraints", *Struct. Eng. Mech.*, **26**(6), 725-739.
Bathe, K.J. and Dvorkin, E.N. (1985), "A Four node plate bending element based on Mindlin/Ressiner plate theory and mixed interpolation", *Int. J. Numer. Meth. Eng.*, **21**, 367-383.
Bathe, K.J., Brezzi, F. and Cho, S.W. (1989), "The MITC7 and MITC9 plate elements", *Comput. Struct.*, **32**, 797-814.
Batoz, J.L. and Lardeur, P. (1989), "A discrete shear triangular nine D.O.F. element for the analysis of thick to very thin plates", *Int. J. Numer. Meth. Eng.*, **28**, 533-560.
Cen, S., Long, Y.Q., Yao, Z.H. and Chiew, S.P. (2006), "Application of the quadrilateral area co-ordinate

method: A new element for Mindlin-Reissner plate", *Int. J. Numer. Meth. Eng.*, **66**, 1-45.

Chen, W.J. and Cheung, Y.K. (2000), "Refined quadrilateral element based on Mindlin/Reissner plate theory", *Int. J. Numer. Meth. Eng.*, **47**, 605-627.

Chen, W.J. and Cheung, Y.K. (2001), "Refined 9-Dof triangular Mindlin plate elements", *Int. J. Numer. Meth. Eng.*, **51**, 1259-1281.

Computers and Structures Inc. (2002), Safe 7.0 User's and Verification Manual.

Computers and Structures Inc. (2002), Sap2000 8.0 User's Manual.

Gruttmann, F. and Wagner, W. (2004), "A stabilized one-point integrated quadrilateral Reissner-Mindlin plate element", *Int. J. Numer. Meth. Eng.*, **61**, 2273-2295.

Hartmann, F. and Katz, C. (2004), *Structural Analysis with Finite Elements*, Springer.

Hughes, T.J.R. (1987), *The Finite Element Method*, Prentice Hall.

Ibrahimbegovic, A. (1992), "Plate quadrilateral finite elements with incompatible modes", *Commun. Appl. Numer. Meth.*, **8**, 497-504.

Ibrahimbegovic, A. (1993), "Quadrilateral finite elements for analysis of thick and thin plates", *Comput. Meth. Appl. Mech. Eng.*, **10**, 195-209.

Jirousek, J., Wroblewski, A. and Szybinski, B. (1995), "A new 12 d.o.f. Quadrilateral element for analysis of thick and thin plates", *Int. J. Numer. Meth. Eng.*, **38**, 2619-2638.

Katili, I. (1993), "A new discrete Kirchhoff-Mindlin element based on Mindlin-reissner plate theory and assumed shear strain fields – Part I: An extended DKT element for thick-plate bending analysis", *Int. J. Numer. Meth. Eng.*, **36**, 1859-1883.

Lyly, M. and Stenbergy, R. (1998), "The stabilized MITC plate bending elements", Computational Mechanics, New Trends and Applications, CINME Press, Barcelona, Spain.

Onate, E., Zienkiewicz, O.C., Suarez, B. and Taylor, R.L. (1992), "A general methodology for deriving shear constrained Reissner-Mindlin plate element", *Int. J. Numer. Meth. Eng.*, **33**, 345-367.

Ozdemir, Y.I., Bekiroglu, S. and Ayvaz, Y. (2007), "Shear locking-free analysis of thick plates using Mindlin's theory", *Struct. Eng. Mech.*, **27**(3), 311-331.

Ozgan, K. and Daloglu Ayse, T. (2007), "Alternative plate finite elements for the analysis of thick plates on elastic foundations", *Struct. Eng. Mech.*, **26**(1), 69-86.

Reddy, J.N. (2000), *Theory and Analysis of Elastic Plates,* Taylor and Francis.

Sheikh, A.H. and Dey, P. (2001), "A new triangular element for the analysis of thick and thin plates", *Commun. Numer. Meth. Eng.*, **17**, 667-673.

Soh, A.K., Cen, S., Long ,Y.Q., Long, Z.F. (2001), "A new twelve DOF quadrilateral element for analysis of thick and thin plates", *Euro. J. Mech. A/Solids*, **20**(2), 299-326.

Sze, K.Y. (2002), "Three-dimensional continuum finite element models for plate/shell analysis", *Pro. Struct. Eng. Mater.*, **4**, 400-407.

Szilard, R. (2004), *Theory and Applications of Plates Analysis of Plates*, John Wiley.

Timoshenko, S. and Krieger, W. (1959), *Theory of Plates and Shells,* McGraw-Hill.

Reismann, H. (1988), *Elastic Plates, Theory and Application*, John Wiley.

Tessler, A. and Hughes, T.J.R. (1985), "A three-node Mindlin plate element with improved transverse shear", *Comput. Meth. Appl. Mech. Eng.*

Urugal, A.C. (1999), *Stress in Plates and Shells 2nd edition*, McGraw-Hill.

Wang, C.M., Reddy, J.N. and Lee, K.H. (2000), *Shear Deformable Beams and Plates*, Elsevier.

Wilson, E.L., Taylor, R.L., Doherty, W. and Ghaboussi, J. (1973), "Incompatible displacement models", *Numer. Comput. Meth. Struct. Mech.*, Academic press.

Zienkiewicz, O.C. and Taylor, R.L. (2000), *The Finite Element Method 5th edition*, 2, Butterworth-Heinemann.